

A Two-sided Model for Droplet Spreading and Evaporation on Semi-confined Geometries

L. A. Hurmez¹, R. Archer¹

¹Department of Engineering Science
 University of Auckland, Auckland 1142, New Zealand

Abstract

In this study we present a numerical simulation for droplet spreading and evaporation on flat surfaces and in a semi-confined geometry. The model takes into account some of the coupled dynamics between the liquid and gas phases in an attempt to develop a coupled model for mass, energy and momentum transport.

The dynamics of the liquid droplet are modelled using the lubrication framework and include the effects of gravity, surface tension and its gradients as well as intermolecular forces and topographical features. The incompressible Navier-stokes equations are used to model the dynamics of the gas phase along with the convection-conduction and convection-diffusion equations to describe energy and vapour transport respectively. The model is solved in COMSOL multiphysics using the finite element method and utilized deformable meshes to couple the solution of the lubrication equation to interface motion.

Introduction

The entrapment of liquid droplets on semi-confined geometries can be encountered in many areas around us with examples that range from industrial spray coating and lubrication to moisture build-up in homes. In many cases, the presence of those droplets is either undesirable or only temporarily required at certain times. Evaporation is one of the most efficient ways of removing sessile droplets in situations where surface topography acts as a physical obstacle to mechanical means.

The dynamics of droplet evaporation on flat and rough surfaces have received a lot of attention in the past three decades both from experimental and a mathematical point of view [1, 2]. In terms of the mathematical models, numerous formulations exist ranging from simple ones that estimate evaporative fluxes based on the droplet's geometry to those that study the dewetting and evaporation of thin film and to those that employ multiphase numerical models based on mass, momentum and energy balances [1, 3, 4].

The lubrication framework is often used to model flow dynamics and evaporation of thin liquid films and droplets. The method has been extensively applied to studying wetting and spreading, dewetting, evaporation, thermally driven flows, surfactant driven flows, flows of various mixtures and flows over topography [4, 5]. The lubrication approximation has also been studied from a pure mathematical sense because of its interesting mathematical formulation [4]. It is based on asymptotic expansions of Navier stokes equations in the limit of thin liquid films and can incorporate micro and macro-scale effects in a compact manner. The resulting equation is a 4th order partial differential equation (PDE) describing the height of the liquid/gas interface in space and time [5]. The lubrication equation is usually solved numerically using methods such as finite element, finite

differences or analytically with further simplifications using perturbation theory and asymptotic analysis [4, 5].

Many of the lubrication models available in the literature and relevant to evaporation are 'one-sided' and do not account for the dynamics of the gas phase for reasons of simplicity and ease of implementation. Although these approximations are appropriate when dealing with gas conditions that do not vary in space and time, they might mask interesting observations in situations where the gas phase dynamics change depending on location, such as in semi-confined geometries. Typical gas conditions of interest can include the velocity, pressure, temperature and moisture profiles.

There have been a few studies [4, 6] looking at setting up and solving two-sided models to account for the gas phase dynamics, most of which were based only on gas diffusion with the assumption of diffusion dominant mode of transport in nearly still conditions [6].

In this work, we attempt to extend those two-sided models by incorporating more physics in the gas phase, namely the mass, energy and momentum equations and accounting for the thermo-physical properties of the gas phase using empirical descriptions. The work uses the lubrication approximation to model the liquid phase over a topographical surface and uses the Arbitrary Lagrangian-Eularian (ALE) method to link the interface height to the gas phase domain. The gas phase is modelled using the incompressible Navier-stokes equations with convection-diffusion and convection-conduction transport of mass and energy, respectively. All the resulting coupled systems of equations are solved in COMSOL multiphysics using the finite element method.

Modelling and physics

Model description

In this simulation we consider a viscous liquid droplet sitting on a heated substrate and surrounded by a moving gas under laminar flow conditions. The dynamics of the liquid droplet of density ρ_{wat} , viscosity μ_{wat} , surface tension σ , molecular weight M and evaporative flux J are modelled using the following lubrication equations [5]:

$$\mu_{wat} \frac{\partial H}{\partial t} + \frac{\partial}{\partial X} \left(\left(\tau + \frac{\partial \sigma}{\partial X} \right) \frac{H^2}{2} \right) - \frac{\partial}{\partial X} \left(\frac{H^3}{3} \frac{\partial P}{\partial X} \right) = - \frac{J \cdot M}{\rho_{wat}} \quad (1)$$

$$P = \rho_{wat} g H - \sigma \frac{\partial^2 (H + S)}{\partial X^2} - \Pi \quad (2)$$

These equations describe the change in height H of the liquid droplet as a function of position X and time t in the presence of gravitational, surface and intermolecular forces. The equations also take into account the effects of local surface tension gradients, the gas shear stresses from the vapour phase τ and the

spatial topography of the substrate S . The term $(J.M/\rho_{\text{wat}})$ in equation (1) corresponds to mass loss due to evaporation with the flux J given by the Hertz-Knudsen relation [1]:

$$J = \alpha \sqrt{\frac{k_b N_a T}{2\pi M}} \left(\frac{P_v}{RT} - c \right) \vec{n} \quad (3)$$

Where α is the accommodation coefficient (\sim unity for water), k_b is Boltzmann's constant, N_a is Avogadro's number, P_v is the saturation vapour pressure at temperature T , R is the universal gas constant, c is the vapour concentration in the gas phase and \vec{n} is the unit normal to the interface.

A disjoining pressure term is used to model the intermolecular forces by assuming the existence of a thin precursor film b that is a fixed percentage of the initial height [7]:

$$\Pi = \left[\left(\frac{b}{H} \right)^n - \left(\frac{b}{H} \right)^m \right] \frac{(n-1)(m-1)\sigma(1-\cos\theta)}{b(n-m)} \quad (4)$$

Here θ is the equilibrium contact angle of the solid/liquid/air interface and (n,m) are positive dimensionless exponents equal to (3,2). The precursor film height is chosen as 2% of the initial droplet height, this provides a reasonable balance between accuracy and numerical efficiency.

The lubrication approximation assumes that the droplet's height is much smaller than its radius, i.e. the approximation is valid for small contact angles. Inclusion of the precursor film and the disjoining pressure term eliminate the divergence issues associated with the lubrication equation and the need for a slip boundary condition at the contact line (the solid/liquid/gas interface).

In this model, we assume that the vapour thrust/recoil effects on the film during evaporation is negligible and thus eliminated from the equation (2). Furthermore it is assumed that the pressure exerted by the gas onto the fluid surface is negligible and is therefore not coupled to the lubrication approximation i.e. gas effects are solely due to the wind force on the liquid/gas interface. The dynamics of the gas phase are modelled using the incompressible Navier-Stokes equations:

$$\nabla \cdot \vec{v} = 0 \quad (5)$$

$$\rho_{\text{mix}} \left(\frac{\partial \vec{v}}{\partial t} + \vec{v} \cdot \nabla \vec{v} \right) = -\nabla p + \mu_{\text{mix}} \nabla^2 \vec{v} \quad (6)$$

Where $\vec{v}=(u,v)$ is the velocity vector and p is the pressure in the gas phase, ρ_{mix} and μ_{mix} are the density and viscosity of the air-vapour mixture at specific temperature and relative humidity respectively. The relative humidity RH is defined by $(cRT/P_v(T))$. We assume here that the force effect due to the weight of the gas is much smaller than the force due to convection and therefore is not included in equation (6).

Evaporation in the gas phase is modelled using the non-conservative form of the convection-diffusion equation and heat is modelled with conduction in the solid and liquid phases and with conduction-convection in the gas phase:

$$\frac{\partial c}{\partial t} + \vec{v} \cdot \nabla c = \nabla \cdot (D \nabla c) \quad (7)$$

$$\rho_{\text{mix}} C_{p\text{mix}} \left(\frac{\partial T}{\partial t} + \vec{v} \cdot \nabla T \right) = \nabla \cdot (k_{\text{mix}} \nabla T) \quad (8)$$

Where D is the temperature dependent diffusion coefficient of vapour in air, C_p is the specific heat of the air-vapour mixture and k_{mix} is the thermal conductivity of the air-vapour mixture at a specific temperature and relative humidity. The thermo-physical properties of the liquid and gas mixtures used in this model are given by [8, 9]

Solution strategy

A special solution strategy is implemented in this simulation to cater for the multiphysical nature of the problem and to reduce the computational efforts by the solver. The lubrication equation is solved in a 1D domain with length of 20mm and 500 cubic Lagrange elements. Then, the solution is coupled to the heat, mass and momentum equations which are solved in a 2D square domain of length 20mm² and \sim 11000 quadratic triangular elements concentrated around the interface boundary. An ALE mesh formulation is used to describe the liquid/air interface in 2D with its motion being described by the solution of the lubrication equation. The liquid and solid domains are distinguished via step functions since the solid phase is fixed and known *a priori*; i.e. the thermo-physical properties of the solid-liquid system are modelled as one bulk system with sharp transition in its properties. The solid phase in this model has the same thermo-physical properties as aluminium.

As evaporation takes place, the temperature, its spatial derivatives, the evaporative flux and the viscous shear stress at the liquid/air interface are linked to the 1D model in order to complete the two-way coupling and calculate volume reductions. The resulting system of PDEs is solved in the COMSOL multiphysics environment using the finite element method.

The 1D-2D model described above is chosen as an example to highlight the need for coupling the gas/liquid physics together in order to model evaporation under dynamic gas conditions. Although this model is appropriate for thin liquid films, it might mask interesting instabilities when modelling droplets as surface tension effects and its interaction with topography are 3-dimensional.

Boundary and Initial conditions

No flow boundary conditions of the Newmann type are used in the lubrication equation with $dH/dX=dP/dX=0$; those are well suited for simulating the spreading of droplets [7]. The momentum, mass and energy boundary conditions in the gas phase are as follows: for the momentum equation, inlet boundary conditions with a constant velocity V_{in} is used on the left boundary of the gas domain and an outlet boundary condition with pressure p_0 and zero viscous stress is prescribed on the right boundary. The upper boundary of the air domain is treated as a solid wall with no slip.

For the diffusion equation, a constant vapour concentration is prescribed on the inlet with $RH_0 * P_v(T_{\text{gas}})/(R * T_{\text{gas}})$ and a convective flux boundary conditions is prescribed on the wall and the outlet. A flux boundary condition is applied to the liquid/air interface as defined by the Hertz-Knudsen relation but used step functions to constrain evaporation to the droplet's radius and prevent the flux from evaporating the precursor film.

For the energy equation, a constant temperature T_{gas} is prescribed at the inlet and convective flux boundary conditions are prescribed on the wall and outlet. A flux discontinuity boundary condition is applied on the liquid/air interface to represent evaporative cooling using $(L_v * M * J)$ with L_v being the latent heat of evaporation of water. In the liquid/solid phases, insulation

boundary conditions are used for the side boundaries and a fixed temperature T_{blm} is prescribed at the lower boundary.

An ALE mesh with deformed frame (x,y) is solved using the solution H and Winslow smoothing. The boundary conditions are $(dx=0, dy=0)$ at the top and bottom boundaries of the domains, $(dx=0)$ at the periphery of the domains and $(dy=H)$ at the liquid/air interface. All the partial differential equations in the gas phase are solved with respect to this deformed frame whereas the lubrication equation is solved relative to an undeformed (reference) frame.

In terms of initial conditions, care must be taken to eliminate discontinuities in the system before solving the complete problem in order to achieve convergence. To do so, the problem is initially decoupled and each equation solved for a few time steps using the previous solution as a starting point. The initial shape for the droplet is that of a spherical cap with radius (R_0) , height $H_0=R_0*\tan(\theta/2)$, and $H(X) = H_0*(1-(X/R)^2)+b$ for $-R<X<R$. Table 1 summarises the settings and conditions used in the model.

Model settings			
R [m]	1.00E-03	V_{in} [m/s]	0.02, 0.2
θ [rad]	$\pi/4$	T_{gas} [K]	293.15
H_0 [m]	4.14e-4	T_{blm} [K]	333.15
b [m]	8.28E-06	RH_0	0.5

Table 1. Boundary and initial settings used in the models

Results and Discussion

Evaporation on a flat surface

Figure 1 show the changes in the interface of the liquid droplet for the first 60 seconds under low flow (left) and high flow (right) conditions. It can be seen that in both cases the droplet's height and radius decrease monotonically as evaporation takes place while the contact angle remains self-similar.

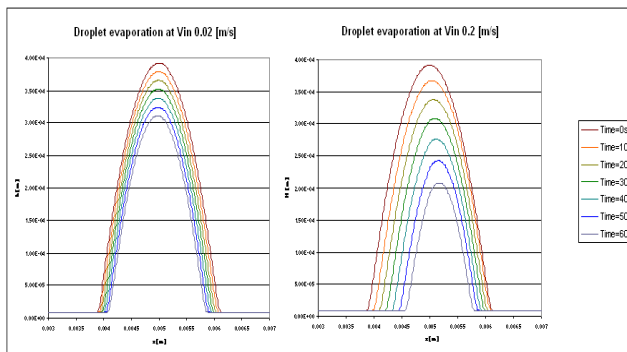


Figure 1. Height profiles of the liquid droplet during the first 60 seconds of evaporation under low (left) and high (right) flow conditions. Parameters used in this simulation: $\theta=\pi/4$, substrate base temperature is 333.15K, inlet gas temperature is 293.15K, inlet gas humidity is 50% and inlet gas velocity is 0.02 and 0.2m/s for the low and high flow cases, respectively.

The figure also shows a faster reduction in the droplet's height under the high flow case as well as a slight shift in the direction of flow. Examining the evaporative fluxes for the two cases at $t=50$ seconds reveal that the flux for the high flow condition is over twice that of the low flow condition; and furthermore, the flux for the high flow condition decreases faster along the length of the droplet than its low flow counterpart (figure 2).

These observations suggest that a convective mode of mass transport is present under the high flow condition and a more diffusive dominant mode of transport is present in the low flow condition as indicated by the mild slop of its evaporative flux. The reduction of mass fluxes with distance is a consequence of mass boundary layer formation which has been suggested elsewhere [11]. The close proximity of the evaporating droplet to the solid surface also increases the evaporative flux as the temperature of the interface approaches that of the solid substrate.

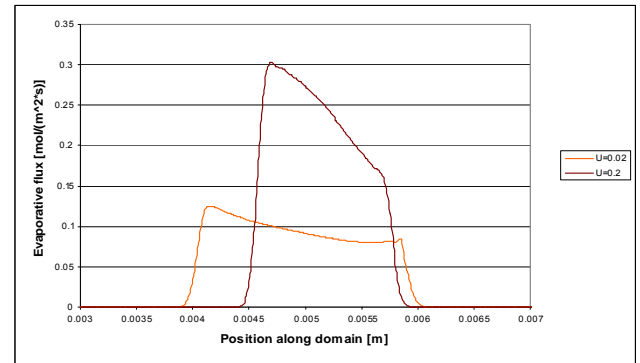


Figure 2. Evaporative flux at $t=50$ seconds for the low and high flow conditions

The slight shift to the right under the high flow case could be explained by the contribution of the wind force at the droplet's interface (figure 3). Figure 3 shows that the shear force at the high flow condition is much larger than its low flow counterpart. The magnitude of this shear force however does reduce with further evaporation as the liquid/gas interface approaches the no-slip boundary of the solid surface (results not shown).

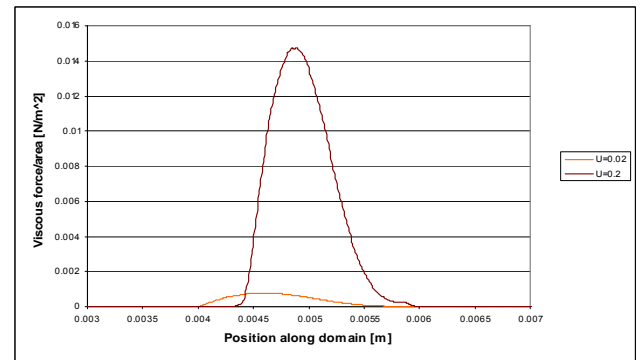


Figure 3. Viscous forces per unit area at $t=50$ seconds for the low and high flow conditions

Evaporation on semi-confined geometry

Step functions are used to construct a pit-like topography with a width of 2.2mm and a depth of 0.3mm. For evaporation in this semi-confined geometry, the droplet is initially positioned close to the right edge of the topography so that the droplet will adhere to that wall at equilibrium rather than spread evenly across the confinement. The droplet is then allowed to spread for 1 second prior to evaporation to ensure convergence of the solution.

Figure 4 shows the height profiles of the droplet and the topography for the first 60 seconds of evaporation. It can be seen that as evaporation takes place, the height of the liquid decreases and the bulk of the fluid translates towards the right wall of the topography due to surface tension forces. The contact angle still remains self-similar under both sides of the topography as this is a consequence of the disjoining pressure term.

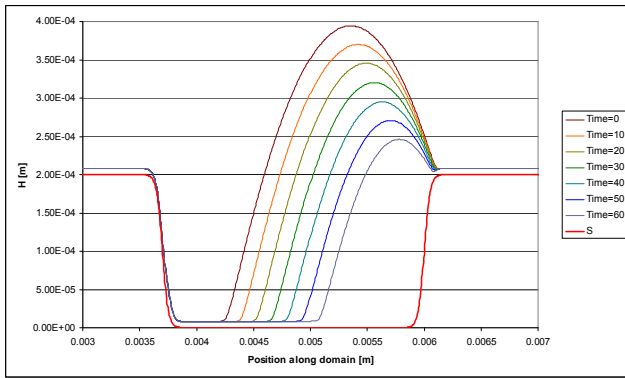


Figure 4. Height profile of the liquid droplet during evaporation on a topography for $t=0-60s$. Parameters used in this simulation: $\theta=\pi/4$, substrate base temperature is 333.15K, inlet gas temperature is 293.15K, inlet gas humidity is 50% and inlet gas velocity is 0.2m/s.

The multiphysical nature of droplet evaporation can be realised when viewing the dynamics of the gas phase in figure 5. Figure 5 show that the incoming laminar flow close to the surface gains heat from the substrate prior to coming in contact with the liquid droplet. This temperature rise is denoted by the upward tilt in the temperature contour lines and the reduction in the relative humidity close to the surface. As the flow reaches the droplet's surface, it gains moisture due to evaporation and convects that moisture away from the droplet's surface. The moisture gain can be seen from the increase in the relative humidity in the gas phase. At this stage, the gas is almost in thermal equilibrium which is indicated by the flattening of the contour lines.

Note that in this example, the gas temperature on the right of the droplet and away from the substrate is less than the minimum required to maintain saturated vapour conditions and so condensation (fog) will appear in the gas phase. This is denoted by the excess relative humidity above 100% in figure 5. If this gas hits a cold surface it will cause a negative evaporative flux and therefore liquid condensation. The simulation of condensation can easily be added to the two-sided model described above by implementing a line function that equals unity when the liquid height is larger than the precursor film and zero otherwise. This function will then replace the step functions multiplied by the diffusive flux boundary condition.

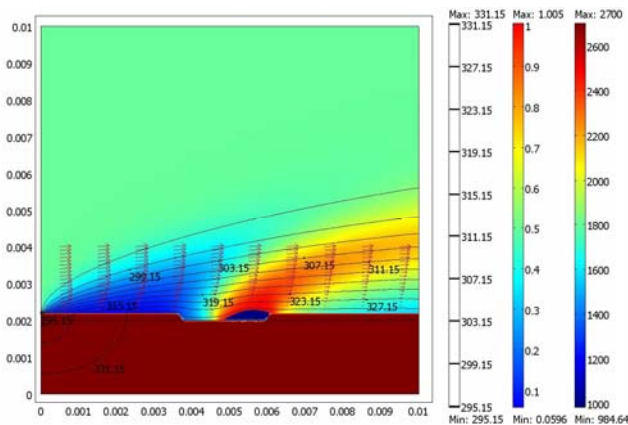


Figure 5. Effects of evaporation on the dynamics in the gas phase for the semi-confined case. Colours in the gas phase denote the fractional change in relative humidity as indicated by the far middle colour bar. Colours in the solid and liquid domains denote the density of the solid and liquid respectively, as indicated by the right colour bar. The arrows denote the velocity field and the contours denote the temperature in the whole domain, as indicated in the left contour bar.

Conclusions

In this work we presented a two-sided model for simulating the spreading and evaporation of a thin liquid droplet on a heated topographical substrate. The dynamics of the liquid phase were modelled using the lubrication approximation while the dynamics of the gas phase were modelled using the standard mass, momentum and energy equations. The phases were then intimately linked using various coupling variables and a deformable mesh formulation.

Numerical simulations on flat and topographical surfaces showed that the dynamics of evaporation is closely related to the conditions on the substrate and in the gas phase. The choice of topography could influence the evaporation conditions and the choice of gas phase properties could affect the rate of evaporation. The numerical simulation also showed that it is possible to predict the location of condensation and with minor improvements, the simulation of liquid build-up on the substrate.

References

1. Cazabat, A.M. & Guéna, G., Evaporation of macroscopic sessile droplets, *Soft Matter*, **6**, 2010, 2591-2612.
2. de Gennes, P.G., Wetting - statics and dynamics, *Reviews of Modern Physics*, **57**, 1985, 827-863.
3. Briones, A.M., et al., Micrometer-sized water droplet impingement dynamics and evaporation on a flat dry surface, *Langmuir*, 2010.
4. Craster, R.V. & Matar, O.K., Dynamics and stability of thin liquid films, *Reviews of Modern Physics*, **81**, 2009, 1131-1198.
5. Oron, A., Davis, S.H., & Bankoff, S.G., Long-scale evolution of thin liquid films, *Reviews of Modern Physics*, **69**, 1997, 931-980.
6. Sultan, E., Boudaoud, A., & Ben Amar, M., Evaporation of a thin film: diffusion of the vapour and Marangoni instabilities, *Journal of Fluid Mechanics*, **543**, 2005, 183-202.
7. Schwartz, L.W., et al., Dewetting patterns in a drying liquid film, *Journal of Colloid and Interface Science*, **234**, 2001, 363-374.
8. Bolz, R.E. & Tuve, G.L., *CRC Handbook of Tables for Applied Engineering Science*, CRC Press, 1973.
9. Tsilingiris, P.T., Thermophysical and transport properties of humid air at temperature range between 0 and 100 °C, *Energy Conversion and Management*, **49**, 2008, 1098-1110.
10. Erbil, H.Y., McHale, G., & Newton, M.I., Drop evaporation on solid surfaces: Constant contact angle mode, *Langmuir*, **18**, 2002, 2636-2641.
11. Incropera, F.P. & DeWitt, D.P., *Fundamentals of heat and mass transfer*, Wiley, 2002.